Monatshefte für Chemie - Chemical Monthly (2020) 151:417–427
https://doi.org/10.1007/s00706-020-02568-8

ORIGINAL PAPER

A facile synthesis, drug-likeness, and in silico molecular docking of certain new azidosulfonamide–chalcones and their in vitro antimicrobial activity

Muhamad Mustafa[1] · **Yaser A. Mostafa**[2]

Received: 25 November 2019 / Accepted: 19 February 2020 / Published online: 31 March 2020

Abstract

New azidosulfonamide–chalcone derivatives were designed and synthesized. Their structures were elucidated by ^{1}H and ^{13}C NMR spectral analyses, in addition to elemental analyses. The synthesized derivatives were tested for their antimicrobial activity against a wide variety of Gram-positive, Gram-negative, and fungal strains. Three azidosulfonamide–chalcones showed relatively broad activity against tested strains. Two compounds exhibited eminent antibacterial activity toward *S. aureus*, *M. luteus*, and *S. marcens* (better than ampicillin trihydrate). The synthesized compounds exhibited moderate activity against *K. pneumonia* and a lower ability to inhibit *E. coli* growth. Among six tested fungal species, the most potent derivatives demonstrated strong activity toward only two of the fungal strains (*T. rubrum* and *G. candidum*). Assessment of drug-likeness, bioavailability, and promiscuity indicated that the compounds are viable drug candidates. In silico molecular docking analysis revealed that the synthesized azidosulfonamide–chalcones successfully occupied pterin-binding site of the dihydropteroate synthase (DHPS), implying that the prepared compounds could exert their activity by the inhibition of the microbial DHPS enzyme. These results provided essential information for the prospective design of more effective antimicrobial compounds.

Graphic abstract

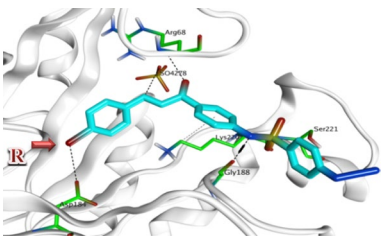

Keywords Azidosulfonamide–chalcones · Antimicrobial · ADMET · Promiscuity · Molecular docking

Introduction

Microbial infections and antibiotic resistance are serious public health threats. Diseases caused by resistant bacteria such as diarrhea, meningitis, respiratory tract infections, sexually transmitted infections, and nosocomial infections are important targets for researchers in the field of antimicrobial agents. In some instances, the misuse of antibiotics leads to uncontrolled bacterial and fungal infections and also to the development of microbial strains, such

Electronic supplementary material The online version of this article (https://doi.org/10.1007/s00706-020-02568-8) contains supplementary material, which is available to authorized users.

✉ Yaser A. Mostafa
y3abdelh@uwaterloo.ca

[1] Medicinal Chemistry Department, Faculty of Pharmacy, Deraya University, Minia, Egypt

[2] Pharmaceutical Organic Chemistry Department, Faculty of Pharmacy, Assiut University, Assiut 71526, Egypt

as MRSA bacterial strains, that till this moment are life-threatening to human beings [1–6]. Compounds containing the sulfonamide group (sulfa drugs, $–SO_2NH_2–$) are widely approved as pharmaceutical agents; they exhibit a wide range of biological activities including anticancer, anti-inflammatory, and antimicrobial [7–11]. Sulfonamides were the first drugs widely employed and systemically used broad-spectrum chemotherapeutics against many bacterial infections. Additionally, it is estimated that sulfonamides account for 16–21% of annual antibiotics usage around the world [11–15]. It is worth mentioning that antimicrobial activities of sulfonamides depend on the substituents and their position on the benzene ring as seen with compounds **1**–**3** (Fig. 1) [16–18]. Additionally, chalcones (α, β-unsaturated carbonyl moiety) as small molecules have been successfully used as potent anti-infective agents. There are several reports about broad-spectrum antimicrobial activity of chalcones bearing hydroxy, alkoxy, or lipophilic groups in their structures (compounds **1** and **4**) (Fig. 1) [16, 19]. Also, it has been reported that linking a chalcone with a sulfonamide moiety (compound **1**) enhances the antimicrobial activity of the prepared derivatives (Fig. 1) [12, 14]; moreover, the literature shows that aryl azides are a common component of bioactive natural products and are considered as a synthetic target due to their feasible and promising applications in click chemistry [4, 17–19]. Agard et al. [20] revealed the great effect of using azides as bioorthogonal chemical reporters on enhancing the biological activity of several molecules such as antibacterial, antiviral, anticancer, COX-2 inhibition, and other biologically active molecules (**2** and **4**–**6**) (Fig. 1) [17, 19, 21, 22]. The antibacterial activity of sulfonamides is attributed to targeting the dihydropteroate synthase enzyme (DHPS) which catalyzes the condensation of 6-(hydroxymethyl)-7,8-dihydropterin-pyrophosphate (DHPPP) and *p*-aminobenzoic acid (PABA) into dihydropteroate (DHPt). As a result, the biosynthesis of dihydrofolic acid is inhibited leading to the prevention of growth and reproduction of microorganisms [23]. Yun et al. [24] reported the crystal structure of *Bacillus anthracis* dihydropteroate synthase (BaDHPS) co-crystallized with sulfathiazole-6-(hydroxymethyl)–7,8-dihydropterin-pyrophosphate (STZ–DHPP) adduct. This adduct was found to occupy both pterin and PABA-binding sites of DHPS. Given these bewildering findings of chalcones, sulfonamides, and aryl azides, along with our interests in developing new potent antimicrobial agents, we herein report the synthesis of sulfonamide–chalcones linked to an azide group as a new approach in developing antimicrobial agents. Also, a selected variety of substituents were implemented on the aryl moiety to test the designed approach of building a hybrid of an azidosulfonamide scaffold and a chalcone scaffold. The effect of the electronic and the lipophilic environments of the selected substituents was studied and compared to the activity of the synthesized azidosulfonamide–chalcones hybrids. Also, the most active compounds **10b** and **10c** were docked into the dihydropteroate synthase active site to assess their ability to perform the same interactions as STZ–DHPP.

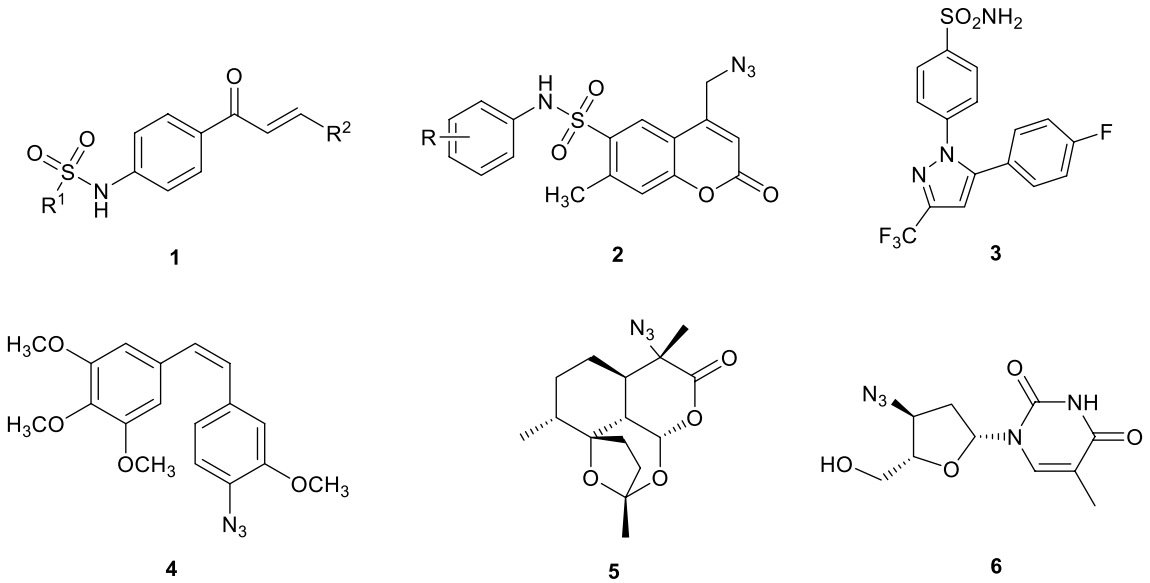

Fig. 1 Structures of some biologically active molecules with a sulfonamide, chalcone, and/or azido group scaffolds

Results and discussion

Chemistry

The facile synthesis of the target azidosulfonamide–chalcones was achieved from the simple and the commercially available sulfanilic acid (compound **7**) according to the reactions sequence shown in Scheme 1. Sulfanilic acid was converted to compound **8** which was used in the next step without further purification. The corresponding azidosulfonamide intermediate (compound **9**) was synthesized from the reaction of compound **8** with *p*-aminoacetophenone in pyridine overnight at room temperature. The target azidosulfonamide–chalcones were then synthesized from compound **9** via its reaction with the appropriate benzaldehyde in a basic medium at the room temperature. The synthesized azidosulfonamide–chalcones **10a**–**10e** were characterized by ^{1}H and ^{13}C NMR, in addition to C, H, N, S elemental analyses (supporting information). The ^{1}H NMR spectra of all the compounds showed a characteristic broad singlet signal at $\delta = 10.8$–10.9 ppm corresponding to the sulfonamide group proton. Also, complex multiplets in the range of 7.0–8.0 ppm were observed corresponding to the aromatic protons of the three phenyl rings. Moreover, the α- and β-H correspond to the –CH=CH– group resonating in the aromatic region as doublets (sometimes overlapped with aromatic protons) with a coupling constant of 15.5 Hz which indicated the formation of the target chalcones with an *E* geometry from their corresponding sulfonamide ketones. The ^{13}C NMR showed a requested number of resonances with distinct signals of C=O, =CH, =C– fragments (supporting information).

Antibacterial activity

All the newly synthesized compounds **9** and **10a**–**10e** were evaluated for their in vitro antibacterial activity against various bacterial strains, including Gram-positive bacteria (*Staphylococcus aureus*, *Micrococcus luteus*, and *Bacillus cereus*), Gram-negative bacteria (*Klebsiella pneumonia*, *Escherichia coli*, and *Serratia marcens*). Ampicillin trihydrate was used as a reference antibacterial agent. The inhibition zone diameters (IZD) in millimeters and the minimum inhibitory concentrations (MIC) in μg/cm^3 of the target compounds are summarized in Table 1. Interestingly, the unsubstituted derivative **10a**, the *p*-Cl derivative **10b**, and the *p*-Br sulfonamide **10c** showed significant activity against *S. aureus* with higher IZD of 23, 27, and 33 mm, respectively, than the reference ampicillin trihydrate of 21 mm. It is worth mentioning that **10b** and **10c** exhibited approximately two- and threefold better MIC values than the reference ampicillin trihydrate. The sulfonamide derivative **10a** showed the same MIC value as the reference compound. Also, **10e** and **10d** exhibited approximately the same ability to inhibit bacterial growth as ampicillin trihydrate. On *M. luteus* bacteria, compound **10c** exhibited highly potent activity with IZD of 29 mm and MIC of 1.50 μg/cm^3, while ampicillin trihydrate exhibited IZD of 18 mm and MIC of 10.08 μg/cm^3. Likewise, **10a** and **10b** showed potent antibacterial activity which was better than ampicillin trihydrate with IZD of 20 and 24 mm, respectively, while the MIC values were 10.10 and 5.47 μg/cm^3, respectively. **10d** and

Scheme 1

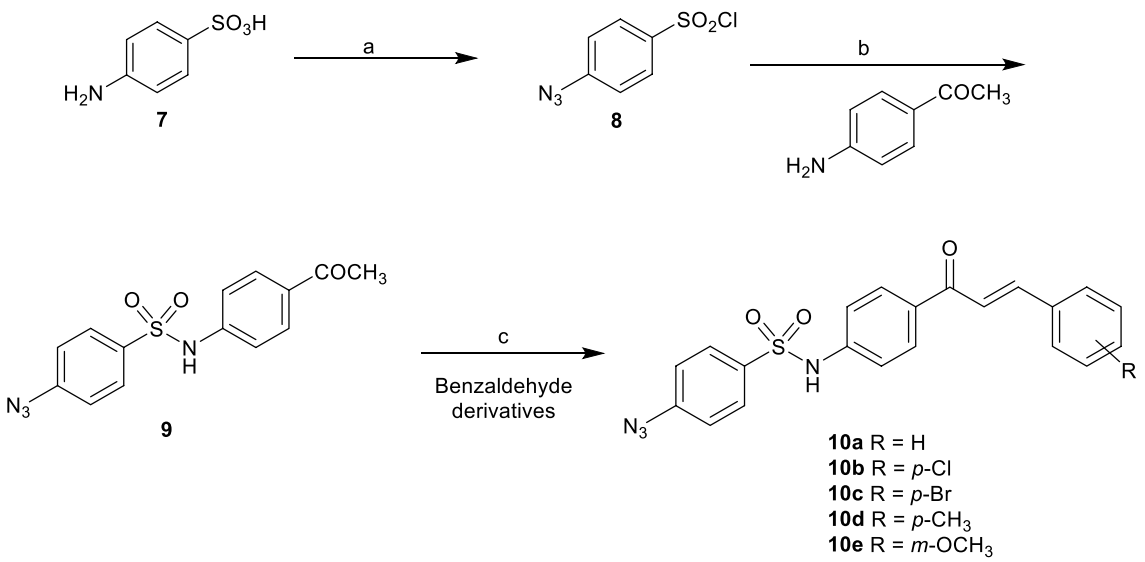

Table 1 The inhibition zone diameters (mm) and the minimum inhibitory concentrations (μg/cm^3) of bacterial species

Compounds	Gram-positive bacteria						Gram −ve bacteria					
	S. aureus		*M. luteus*		*B. cereus*		*K. pneumonia*		*E. coli*		*S. marcens*	
	IZD	MIC	IZD	MIC	IZD	MIC	IZD	MIC	IZD	MIC	IZD	MIC
9	17	15.80	15	31.60	13	31.60	8	> 50	8	> 50	10	> 50
10a	23	5.05	20	10.10	17	40.41	13	40.41	11	40.41	14	20.20
10b	27	2.73	24	5.47	20	21.90	17	21.90	18	10.95	17	5.47
10c	33	1.50	29	1.50	22	24.10	19	12.05	20	6.05	17	6.02
10d	22	10.45	18	20.90	21	41.81	11	> 50	14	20.90	11	41.81
10e	20	10.85	17	43.41	18	43.41	10	> 50	12	21.70	10	43.41
Ampicillin trihydrate	21	5.04	18	10.08	30	2.52	20	10.08	33	1.25	18	5.04

IZD inhibition zone diameter, *MIC* minimal inhibitory concentration

10e showed approximately the same IZD as the reference compound. However, MIC values showed a drastic increase in comparison to ampicillin trihydrate. All the synthesized derivatives showed relatively moderate activity on *B. cereus* when compared to the reference compound. On Gram-negative bacteria, **10c** showed approximately the same IZD and MIC value as that of ampicillin trihydrate on *K. pneumonia*. **10b** and **10c** exhibited potent IZD and MIC value on *S. marcens* bacteria. The reference ampicillin trihydrate was able to inhibit the growth of *E. coli* significantly more than all the synthesized sulfonamides. These results indicated that compounds bearing electron-withdrawing groups showed better antibacterial activity than the derivatives bearing electron-donating groups. Also, the MIC of the key intermediate **9** was so much enhanced (four times lower) upon its conversion to the first azidosulfonamide–chalcone **10a** which showed better MIC values compared to ampicillin trihydrate on both *S. aureus* and *M. Luteus*.

Antifungal activity

The synthesized azidosulfonamide–chalcones were tested for their in vitro antifungal activity against six different pathogenic fungi including (*Trichophyton rubrum*, *Candida albicans*, *Fusarium oxysporum*, *Penicillium chrysogenum*, *Geotrichum candidum*, and *Aspergillus niger*). The screening was performed using the twofold serial dilution method using fluconazole as the reference drug (Table 2). All the derivatives showed moderate to potent antifungal efficiency except **10b** and **10c** which showed a significantly potent antifungal potency against *T. rubrum*. The *p*-Cl derivative **10b** and the *p*-Br sulfonamide **10c** exhibited higher IZD of 25 and 28 mm, respectively, when compared to the reference fluconazole (24 mm). Favorably, **10a**, **10b**, and **10c** showed the best MIC values of 10.10, 2.73, and 3.01 μg/cm^3, respectively (fluconazole: 15.30 μg/cm^3). Regarding *C. albicans*, all the derivatives showed mild activities, however, with less potency when compared to the reference fluconazole. The chalcone derivative **10c** showed a strong ability to inhibit the growth of *G. candidum* exhibiting considerable MIC value (approximately twice that of fluconazole). Similar to the antibacterial activity, **10a**–**10e** showed better antifungal activity than their corresponding intermediate compound **9**. Also, derivatives bearing electron-withdrawing groups (**10b** and **10c**) exhibited higher antifungal potency than derivatives carrying electron-donating functionalities (**10d** and

Table 2 The inhibition zones (mm) and the minimum inhibitory concentrations (μg/cm^3) of fungal species

Compounds	Tested fungi											
	T. rubrum		*C. albicans*		*F. oxysporum*		*P. chrysogenum*		*G. candidum*		*A. niger*	
	IZD	MIC	IZD	MIC	IZD	MIC	IZD	MIC	IZD	MIC	IZD	MIC
9	10	15.80	10	> 50	< 2	N.T.	< 2	N.T.	8	> 50	< 2	N.T.
10a	19	10.10	13	> 50	< 2	N.T.	< 2	N.T.	11	40.40	< 2	N.T.
10b	25	2.73	15	43.80	< 2	N.T.	< 2	N.T.	18	10.95	< 2	N.T.
10c	28	3.01	18	48.20	< 2	N.T.	< 2	N.T.	20	6.02	< 2	N.T.
10d	17	20.90	12	> 50	< 2	N.T.	< 2	N.T.	14	20.90	< 2	N.T.
10e	12	21.70	11	> 50	< 2	N.T.	< 2	N.T.	11	43.41	< 2	N.T.
Fluconazole	24	15.30	28	1.91	26	N.T.	23	N.T.	22	3.83	18	N.T.

IZD inhibition zone diameter, *MIC* minimal inhibitory concentration

10e). None of the tested compounds showed any notable antifungal activity against either *F. oxysporum*, *P. chrysogenum*, or *A. niger*. A Venn diagram was created for all compounds exhibiting potent activity against Gram-positive, Gram-negative, and fungi strains [1]. The diagram showed that compounds **10b** and **10c** shared a broad-spectrum antimicrobial activity profile (Fig. 2).

Drug-likeness

Lipinski parameters [25, 26] (drug-likeness or ADMET properties) were calculated by Swiss ADME predictor software (http://www.swissadme.ch/) [27]. These parameters include molecular weight (MW), number of rotatable bonds (nrotb), hydrogen-bond acceptors (HBA) and donors (HBD), lipophilicity (ilogP), and topological polar surface area (TPSA) of the newly synthesized compounds as candidate drugs (Table 3). Prediction of these ADMET properties helps in predicting the transport properties of the molecules through the membranes such as blood–brain barrier (BBB) and gastrointestinal tract (GI tract). If the compounds failed to obey two or more of these drug-likeness parameters, there would be a high possibility of their poor bioavailability. All the newly synthesized compounds **9** and **10a**–**10e** were characterized by having 6 H-bond acceptor atoms and one H-donor (except compound **10e** has 7 H-bond acceptors); these centers helped in H-bond formation and, therefore, enhanced water solubility. Additionally, compounds **10a**–**10d** displayed seven rotatable bonds while **10e** showed eight rotatable bonds. The importance of these rotatable bonds is to boost the adaptation and the flexibility of the compound leading to creating more interactions within the active site. Another important physicochemical parameter is lipophilicity or partition coefficient (iLogP);

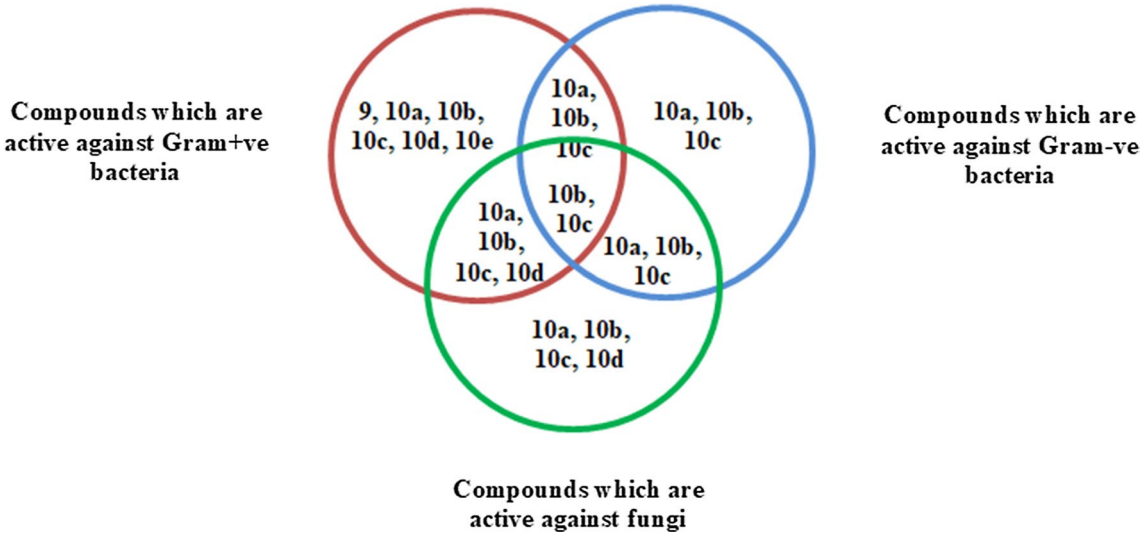

Fig. 2 Venn diagram of the antimicrobial activity relation of synthesized compounds

Table 3 Calculated drug-likeness parameters

Compound	MW/g mol^{-1}	Lipinski parameters						Water solubility Silicos-IT class
		HBA	HBD	Nrotb	TPSA/Å^2	iLogP	*F*	
9	316.34	6	1	5	121.37	2.11	0.56	Moderately soluble
10a	404.44	6	1	7	121.37	2.49	0.56	Moderately soluble
10b	438.89	6	1	7	121.37	2.98	0.56	Poorly soluble
10c	483.34	6	1	7	121.37	3.09	0.56	Poorly soluble
10d	418.47	6	1	7	121.37	2.71	0.56	Moderately soluble
10e	434.47	7	1	8	130.60	2.19	0.56	Moderately soluble
Drug lead-like properties	≤500	≤10	≤5	≤10	≤140	≤5		

MW molecular weight, *HBA* H-bond acceptor, *HBD* H-bond donor, *nrotb* no. of rotatable bonds, *TPSA* topological polar surface area, *iLogP* *n*-octanol/water partition coefficient, *F* Abbott bioavailability scores

compounds having values less than − 0.5 will have poor dissolution in lipids and will not be able to penetrate cell membranes. The prepared compounds were found to have iLogP values between 2.19 and 3.09 which indicated the probability of a good penetration through cell membranes and hence better bioavailability. Likewise, TPSA and MW affect the transportation of the molecules through the biological membranes. Generally, compounds with MW below 500 g/mol and TPSA less than 140 Å^2 could transfix through membranes easily, rapidly and subsequently will have less undesirable side effects. Moreover, assessment of the bioactivity score (F) of the new compounds using Swiss ADMET showed their substantial bioavailability (score above zero) and hence a higher probability of medicinal impact and biological activities in clinical trials [28]. Fortunately, all these calculations did not violate any of the Lipinski rules and met the bioavailability requirements (Table 3).

Table 4 The pScore and inDrug findings from Badapple data base

Cpd	Scaffold	pScore	inDrug
9 and **10a–10e**	Sulfonamide **11**[a]	257	True
10a–e	Chalcone **12**[a]	785	True
10a–e	Compound **13**[a]	63	False

pScore values advisory: < 100 (low), means no indication; 100–300 (moderate), means weak indication of promiscuity; > 300 (high), means strong indication of promiscuity; inDrug results: true, means it was found in the drug data base; false, means not found

[a]Structures of scaffolds are shown in Fig. 3

Promiscuity

Pan assay interference compounds (PAINS) analysis is used to illustrate how frequent a compound is used in many biochemical high-throughput drug discovery screens, thus could be promising start points for further drug development. Promiscuity of the prepared compounds was screened by bioactivity data-associative promiscuity pattern learning engine (Badapple: http://pasilla.health.unm.edu/tomcat/badapple/badapple) (Table 4) [29]. PAINS analysis revealed interesting findings which are: first, both the key intermediate **9** and the final compounds **10a–10e** shared a common scaffold, compound **11** (Fig. 3) with a moderate pScore value accompanied with a "True" result inDrug database; second, another scaffold, compound **12** (Fig. 3) embedded in the final compounds was found to have pScore higher than 300 with a "True" result inDrug database. Both of these findings heighten our compound promiscuity and drug-likeness probability; Finally, a third scaffold, compound **13**, was generated from PAINS engine with a pScore below 100 and a "False" finding inDrug database indicating its absence in the drug database.

In silico molecular docking analysis

To further rationalize the potent antimicrobial activity of the prepared compounds, molecular docking was performed in the dihydropteroate synthase binding site. The PDB code (3TYE) of the published crystal structure was obtained

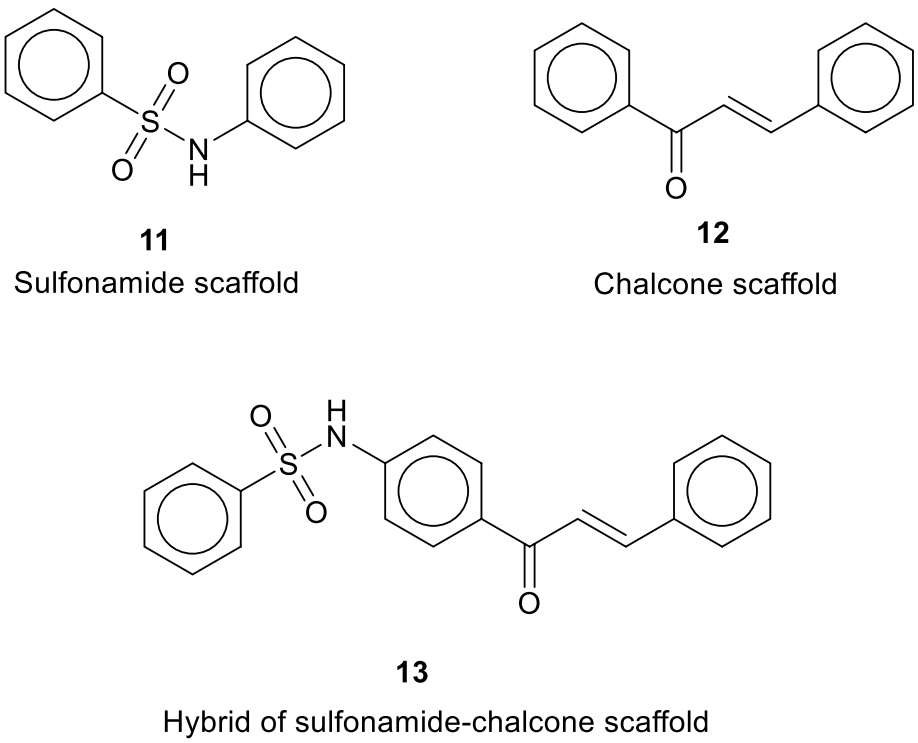

Fig. 3 Scaffolds generated from promiscuity PAINS database

from Protein Data Bank [24]. To assess the docking performance, the co-crystallized ligand STZ–DHPP was self-docked into the active site showing an acceptable RMSD value of 0.7920 Å (Fig. 4a). The docked compounds showed several favorable van der Waals and hydrogen bonding interactions with several key amino acids inside the active site (Table 5, Fig. 4). The docking pose of the *p*-Cl azidosulfonamide–chalcone **10b** (magenta) showed a hydrogen bonding interaction between the chlorine atom and Asn120 (− 2.09 kJ/mol) (Fig. 4b).

The sulfonamide proton showed a hydrogen bond with Gly188 while the sulfonamide oxygen showed another hydrogen bond with Ser221 (− 22.59 and − 2.51 kJ/mol, respectively). Phe189 and Lys220 made H···π with the sulfonamide phenyl ring (− 1.67 and − 1.25 kJ/mol, respectively). The *p*-Br azidosulfonamide–chalcone **10c** (cyan) which exhibited the highest antimicrobial activity showed several interactions inside the active site (Fig. 4c). Asn120 and Asp184 showed two favorable hydrogen bonds with the bromine atom. Also, the sulfonamide group showed two hydrogen bonding interactions with Ser221 and Gly188 (− 2.09 and − 19.24 kJ/mol, respectively). Also, the sulfonamide phenyl ring showed H···π interaction with Lys220 with interaction energy of − 1.25 kJ/mol interestingly, the methylene proton of the chalcone moiety showed a hydrogen bond with sulfate residues present in the dihydropteroate synthase active site. The role of chalcone moiety was observed again with a hydrogen bond between the carbonyl oxygen and Arg68. Both of the docked sulfonamides (**10b** and **10c**) successfully and completely occupied the receptor active site and were oriented almost identical to the co-crystallized ligand STZ–DHPP (Fig. 4d). Moreover, **10b** and **10c** showed several hydrophobic interactions with Arg68, Pro69, Arg254, Lys220, Gly188, Ser221, and Pro193 amino acids. These interesting interactions of the docked derivatives indicated their substantial ability to occupy the pocket preventing the substrate STZ–DHPP from binding, leading to the inhibitory activity of the prepared compounds against DHPS. All these essential interactions may account for the potent antimicrobial effects of the prepared derivatives.

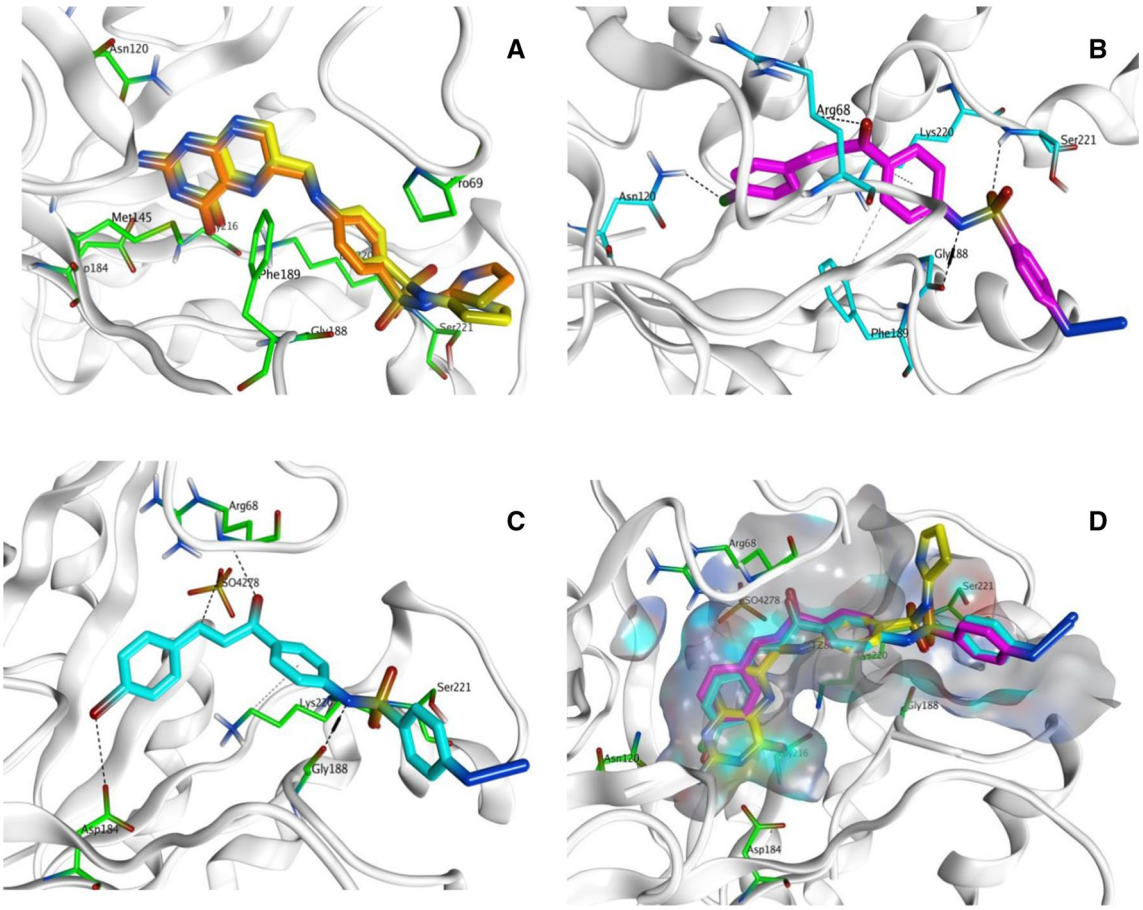

Fig. 4 Presumptive binding modes of the studied compounds. **a** Self-docking of STZ–DHPP with BaDHPS active site; **b** docking pose of compound **10b** (magenta); **c** docking pose of compound **10c** (cyan); **d** presumptive binding modes of compound **10b** (magenta), compound **10c** (cyan), and STZ–DHPP (yellow). All the docked sulfonamides and STZ–DHPP are in stick representation (PDB code: 3TYE)

Table 5 Energy scores (kJ/mol) and binding interactions for the co-crystallized ligand (STZ–DHPP) and the top potent compounds **10b** and **10c**, within dihydropteroate synthase active site

Compound	Energy score, *S*/kJ mol^{-1}	Ligand–receptor interactions		
		Residue	Type	Length/Å
STZ–DHPP	− 34.22	Asn120	Hydrogen bond	2.74
		Asp184	Hydrogen bond	3.02
		Lys220	Hydrogen bond	3.31
		Ser221	Hydrogen bond	3.04
		Lys220	H···π	4.09
		Asn120	Hydrogen bond	3.10
10b	− 29.37	Ser221	Hydrogen bond	3.02
		Gly188	Hydrogen bond	2.87
		Lys220	H···π	4.12
		Phe189	H···π	4.32
		SO_4^{2-}	Hydrogen bond	2.51
		Asn120	Hydrogen bond	3.08
10c	− 30.08	Asp184	Hydrogen bond	3.22
		Ser221	Hydrogen bond	3.11
		Gly188	Hydrogen bond	2.81
		Lys220	H···π	4.28

Conclusion

To summarize, a series of azidosulfonamide–chalcone derivatives were successfully designed and synthesized. The antimicrobial screening and the computational analysis were performed on the prepared derivatives. All the derivatives exhibited moderate to strong antimicrobial activities against most of the tested microbial strains. Among the synthesized compounds and the reference ampicillin trihydrate, the sulfonamide derivatives **10a**, **10b**, and **10c** showed the best antibacterial activity on *S. aureus* and *M. luteus* bacteria. The *p*-Br derivative **10c** exhibited strong antifungal activity on *T. rubrum*, which was better than the reference fluconazole. It is worth noticing that the derivatives carrying electron-withdrawing groups (**10b** and **10c**) exhibited higher antimicrobial activity over the derivatives carrying electron-donating groups (**10d** and **10e**). Moreover, promiscuity analysis revealed that all the new derivatives **10a**–**10e** in addition to their key intermediate **9** shared a common scaffold with strong pScore (> 300) which was also found to be commonly used in the drug database. Finally, in silico screening of the new derivatives showed considerable interactions within the dihydropteroate synthase binding site. From all these interesting findings, this new approach seems to be a promising start point for further investigations, and these compounds resemble proper candidates as potent antimicrobial agents.

Experimental

The experimental methods, reagents, solvents, ^{1}H and ^{13}C NMR data and spectra are listed and described in the supporting information, in addition to elemental analyses (C, H, N, and S) and melting points for all new compounds. All starting materials and reagents were obtained from Alpha Aesar Chemical Company® and Sigma-Aldrich Chemicals Company®. Pyridine was distilled from KOH pellets, thionyl chloride was freshly distilled under reduced pressure, and toluene was distilled over CaH under reduced pressure. Silica gel chromatography was performed using silica gel obtained from Fluka™. Melting points were recorded on Electrothermal™ Melting point apparatus. ^{1}H and ^{13}C NMR spectra were recorded in DMSO-d_6 on a JEOL ECA-500 II using TMS as internal standard (chemical shifts in ppm) and chemical shifts for ^{13}C spectra are relative to the residual solvent peak ($\delta = 39.5$ ppm, central peak). Microanalyses determined for C, H, N, and S were within ± 0.4 of theoretical values.

4-Azidobenezenesulfonyl chloride (8)

To a solution of 5.8 g sodium carbonate in 200 cm^3 H_2O, 250 g sulfanilic acid (**7**) was added portion-wise with vigorous stirring. To the resultant solution, 8.4 g sodium nitrite was added and stirring was continued till complete dissolution of sodium nitrite. This step was followed by portion-wise addition of a solution of 14 cm^3 concentrated HCl in 30 cm^3 H_2O with vigorous stirring in an ice bath to maintain the reaction between 0 and 5 °C. A white precipitated was obtained, separated by suction, and washed with about 80 cm^3 of cold water. The precipitate solid was then dispersed in 40 cm^3 of cold water, whereupon a solution of sodium azide (8 g in 20 cm^3 water) was added portion-wise till the evolution of N_2 ceased. After that, 30 g NaCl was added to salt out. The resulting precipitate was filtered off and dried in vacuum to yield a yellowish-white precipitate. 5 g of the resultant azido derivative was dissolved in 20 cm^3 thionyl chloride and 3 drops of DMF and heated till boiling for 30 min. After completion of the reaction, the excess $SOCl_2$ was removed under vacuum and the residue was extracted with 100 cm^3 ether. The etherial extract was evaporated under vacuum to afford 4-azidobenzene sulfonyl chloride (**8**) as a yellowish-white solid. Yield: 4.1 g (76%); m.p.: 59–61 °C [7].

4-Azido-*N*-(4-acetylphenyl)benzenesulfonamide (9, $C_{14}H_{12}N_4O_3S$) To a solution of **8** (0.01 mmol), *p*-aminoacetophenone was added (0.01 mmol) in 1 cm^3 dry pyridine at 0 °C. After addition, the reaction was stirred for 16 h at room

temperature, and then pyridine was azeotropically removed with toluene under vacuum. The residue was dissolved in EtOAc, washed with H_2O and brine. The resultant compound was then dried (Na_2SO_4), filtered, and concentrated under vacuum. Purification was achieved using recrystallization from EtOH which provided **9** as a pink solid (89%). M.p.: 94-96 °C; ^{1}H NMR (DMSO-d_6, 500 MHz): $\delta = 10.87$ (s, 1H, $SO_2N\underline{H}$), 7.84–7.81 (m, 4H, Ar–H), 7.27 (app. d, 2H, $J = 6.5$ Hz, Ar–H), 7.19 (app. d, $J = 9$ Hz, 2H, Ar–H), 2.45 (s, 3H, $COCH_3$) ppm.

General procedure for the synthesis of sulfonamide–chalcones 10a–10e

To a solution of **9** (0.5 mmol) and appropriate benzaldehydes (0.5 mmol) in 10 cm^3 EtOH, aq. NaOH (1 mmol) was added drop-wise with constant stirring for 30 min during which a yellow cake was formed. It was then kept overnight at room temperature. The solid cake so obtained was acidified with dilute HCl, and solid obtained was filtered, washed with 2% $NaHCO_3$, and again with H_2O and brine. The resultant compound was then purified with flash chromatography to get target compounds **10a**–**10e**.

***N*-[4-(3-Phenylacryloyl)phenyl]-4-azidobenzenesulfonamide (10a, $C_{21}H_{16}N_4O_3S$)** Purification was achieved using flash chromatography (ethyl acetate/hexane, 3:7) which provided **10a** as a bright yellow solid (87%). M.p.: 283–285 °C; ^{1}H NMR (DMSO-d_6, 500 MHz): $\delta = 10.93$ (br s, 1H, $SO_2N\underline{H}$), 8.05 (d, 2H, $J = 9$ Hz, Ar–H), 7.98–7.83 (m, 5H, 4 Ar–H, =CH–), 7.67 (d, $J = 15$ Hz, 1H, =CH–), 7.45–7.43 (m, 3H, Ar–H), 7.29–7.23 (m, 4H, Ar–H) ppm; ^{13}C NMR (DMSO-d_6, 125 MHz): $\delta = 187.5$ (C=O), 144.5, 143.5, 142.6, 135.4, 134.7, 132.5, 130.6 (2 CH_{Ar}), 128.9–128.7 (6 CH_{Ar}), 121.8 (CH_{Ar}), 120 (2 CH_{Ar}), 118.1 (2 CH_{Ar}) ppm.

***N*-[4-[3-(4-Chlorophenyl)acryloyl]phenyl]-4-azidobenzenesulfonamide (10b, $C_{21}H_{15}ClN_4O_3S$)** Purification was achieved using flash chromatography (ethyl acetate/hexane, 2:8) which provided **10b** as a bright yellow solid (77%). M.p.: > 300 °C; ^{1}H NMR (DMSO-d_6, 500 MHz): $\delta = 10.92$ (br s, 1H, $SO_2N\underline{H}$), 8.06 (d, 2H, $J = 9$ Hz, Ar–H), 7.87–7.83 (m, 5H, 4 Ar–H, =CH–), 7.65 (d, $J = 15$ Hz, 1H, =CH–), 7.50 (d, 2H, $J = 9$ Hz, Ar–H), 7.29–7.23 (m, 4H, Ar–H) ppm; ^{13}C NMR (DMSO-d_6, 125 MHz): $\delta = 187.4$ (C=O), 144.5, 142.3, 142, 135.1, 134.9, 133.6, 132.5, 130.3 (4 CH_{Ar}), 128.8 (4 CH_{Ar}), 122.5 (CH_{Ar}), 119.9 (2 CH_{Ar}), 118.1 (2 CH_{Ar}) ppm.

***N*-[4-[3-(4-Bromophenyl)acryloyl]phenyl]-4-azidobenzenesulfonamide (10c, $C_{21}H_{15}BrN_4O_3S$)** Purification was achieved using flash chromatography (ethyl acetate/hexane, 2.5:7.5) which provided **10c** as a yellow solid (83%). M.p.: > 300 °C; ^{1}H NMR (DMSO-d_6, 500 MHz): $\delta = 10.92$ (br s, 1H, $SO_2N\underline{H}$), 7.88 (d, 2H, $J = 16$ Hz, =CH–), 7.85–7.80 (m, 4H, 4 Ar–H), 7.65–7.62 (m, 3H, 2 Ar–H, =CH), 7.25–7.17 (m, 4H, Ar–H) ppm; ^{13}C NMR (DMSO-d_6, 125 MHz): $\delta = 187.3$ (C=O), 144.3, 144.3, 142.6, 141.9, 135.5, 134, 132, 131.7, 130.7, 130.5, 129.7, 128.7 (2 CH_{Ar}), 122.5 (CH_{Ar}), 119.9 (2 CH_{Ar}), 118.1 ppm.

***N*-[4-[3-(4-Methylphenyl)acryloyl]phenyl]-4-azidobenzenesulfonamide (10d, $C_{22}H_{18}N_4O_3S$)** Purification was achieved using flash chromatography (ethyl acetate/hexane, 1:9) which provided **10d** as a pale yellow solid (69%). M.p.: 297–299 °C; ^{1}H NMR (DMSO-d_6, 500 MHz): $\delta = 10.87$ (br s, 1H, $SO_2N\underline{H}$), 8.03 (app. d, 2H, $J = 6.5$ Hz, 2 Ar–H), 7.84–7.81 (m, 5H, 4 Ar–H, =CH–), 7.64 (d, 1H, $J = 15.5$ Hz, =CH–), 7.28-7.18 (m, 4H, Ar–H), 2.49 (s, 3H, CH_3 overlapping H_2O signal) ppm; ^{13}C NMR (DMSO-d_6, 125 MHz): $\delta = 187.5$ (C=O), 144.5, 143.6, 142.1, 135.2, 132, 130.1, 129.8 (2 CH_{Ar}), 129.5, 128.8 (2 CH_{Ar}), 120.7 (CH_{Ar}), 119.9 (2 CH_{Ar}), 118.1 (2 CH_{Ar}), 26.4 (CH_3) ppm.

***N*-[4-[3-(3-Methoyphenyl)acryloyl]phenyl]-4-azidobenzenesulfonamide (10e, $C_{22}H_{18}N_4O_4S$)** Purification was achieved using flash chromatography (ethyl acetate/hexane, 1.5:8.5) which provided **10e** as a yellow solid (73%). M.p.: > 300 °C; ^{1}H NMR (DMSO-d_6, 500 MHz): $\delta = 10.92$ (br s, 1H, $SO_2N\underline{H}$), 8.04 (d, 2H, $J = 9$ Hz, 2 Ar–H), 7.87–7.81 (m, 5H, 4 Ar–H, =CH–), 7.63 (d, 1H, $J = 15.5$ Hz, =CH–), 7.38 (d, $J = 7.5$ Hz, 1H, Ar–H), 7.34 (t, $J = 8$ Hz, 1H, Ar–H), 7.27–7.22 (m, 5H, Ar–H), 7.00 (dd, $J = 2.0$, 1.5 Hz, 1H, Ar–H), 3.82 (s, 3H, OCH_3) ppm; ^{13}C NMR (DMSO-d_6, 125 MHz): $\delta = 187.4$ (C=O), 159.6, 144.3, 143.4, 143.2, 136.1, 135.6, 132.3, 130.3 (2 CH_{Ar}), 129.8, 128.7 (2 CH_{Ar}), 122.1, 121.5, 119.9 (2 CH_{Ar}), 118.1 (2 CH_{Ar}), 116.6 (CH_{Ar}), 113.2 (CH_{Ar}), 55.3 (OCH_3) ppm.

Biological activity

Bacterial and fungal cultures were obtained from Assiut university microbiology center (AUMC), Assiut University. Six bacterial strains, three Gram-positive species: *Staphylococcus aureus* (*S. aureus*: AUMC, B-54), *Micrococcus luteus* (*M. luteus*: AUMC, B-224), and *Bacillus cereus* (*B. cereus*: AUMC, B-100), three Gram-negative species: *Klebsiella pneumonia* (*K. pneumonia*: AUMC, B-178), *Escherichia coli* (*E. coli*: AUMC, B-221), and *Serratia marcens* (*S. marcens:* AUMC, B-89) were used to test antibacterial activity of synthesized compounds; and six fungal strains: *Trichophyton rubrum* (*T. rubrum*: AUMC 1145), *Candida albicans* (*C. albicans*: AUMC 421), *Fusarium oxysporum* (*F. oxysporum*: AUMC 208), *Penicillium chrysogenum* (*P. chrysogenum*: AUMC 278), *Geotrichum candidum* (*G. candidum*:

AUMC 228), and *Aspergillus niger* (*A. niger*: AUMC 3364) according to the agar cup diffusion method.

Antibacterial activity

Cell suspension of test bacterial strains was prepared from 48-h-old cultures previously grown on nutrient agar (NA) in 15-cm-diameter plates, which were seeded using 0.1 cm^3 of diluted organism. 100 mm^3 of tested compounds (**10a**–**10e**: 100 µg/cm^3 of DMSO), negative control (DMSO), and positive control (ampicillin trihydrate [31]) was added to specified wells. The seeded plates were incubated at 35 ± 2 °C for 24 h; after that, the inhibition zone diameter was measured in millimeters (Table 1). Also, minimum inhibitory concentrations (MICs) were determined for the most active compounds using twofold dilution method (Table 1).

Antifungal activity

Spore suspension of test fungi were grown on sterile malt extract broth agar (MEB), Sabouraud agar (SA), and/or potato dextrose agar (PDA) according to test fungal species with final spore concentration of (5×10^4 spores/cm^3) in sterile Petri dishes (9 cm in diameter). Plates were inoculated with 1 cm^3 of spore suspension and were shaken gently to homogenize the inoculum. Test compounds (**10a**–**10e**: 100 mm^3 of 100 µg/cm^3 of DMSO), negative control (DMSO), and positive control (fluconazole [31]) were added to specified wells in triplicate and plates were incubated at 28 ± 2 °C for 1–7 days according to the test fungi used. The diameter of inhibition zones (in mm) and MICs (µg/cm^3) of most active compounds were determined using twofold dilution method (Table 2).

Calculation of Lipinski parameters

Pharmacokinetics and drug-likeness prediction for all the newly synthesized compounds were performed by online tool SwissADME predictor software (http://www.swissadme.ch/) made by Swiss Institute of Bioinformatics (https://www.sib.swiss/). In the present study, Lipinski parameters (MW, molecular weight; HBA, H-bond acceptor; HBD, H-bond donor; TPSA, topological polar surface area; iLogP, *n*-octanol/water distribution coefficient), number of rotatable bonds (nrotb), Abbott bioavailability score (*F*), water solubility, and membrane permeability parameters were calculated as shown in Table 3.

Promiscuity analysis

A pan assay interference compound (PAINS) analysis new compound was screened by bioactivity data-associative promiscuity pattern learning engine (Badapple: http://pasilla.health.unm.edu/tomcat/badapple/badapple), data are shown in Table 4 and structures of scaffolds are shown in Fig. 3.

Molecular docking analysis

In silico molecular modeling and visualization processes were performed using Molecular Operating Environment (MOE 2014.0901, Chemical Computing Group, Montreal, QC, Canada). The co-crystal structure was downloaded from the RCSB Protein Data Bank (PDB code 3TYE). First, the compounds were prepared with the standard protocol designated in MOE 2014.09. However, the energy of the docked structures was minimized using MMF94FX force field with gradient RMS of 0.0001 kcal/mol and then the protein structure was prepared using the MOE LigX protocol. To validate the docking study at the dihydropteroate synthase active site, the co-crystallized ligand STZ–DHPP was re-docked into the binding site using the same set of parameters as described above. The RMSD of the best docked pose was 0.7920 Å and the binding score was − 34.22 kJ/mol. The ligands were then docked in the binding site using the alpha triangle placement method. The refinement was carried out using force field and was scored using the affinity ΔG scoring system. The resulting docking poses were visually inspected, and the poses of the lowest binding free energy value and with the best hydrophobic, H-bonding, and electrostatic interactions within the binding pocket of target protein were considered to figure out the antibacterial activity (Table 5, Fig. 4) [30].

References

1. Ahmed N, Konduru NK, Owais M (2019) Arab J Chem 12:1879
2. Payne DJ, Gwynn MN, Holmes DJ, Pompliano DL (2007) Nat Rev Drug Discov 6:29
3. Sivakumar PM, Ganesan S, Veluchamy P, Doble M (2010) Chem Biol Drug Des 76:407
4. Phetsang W, Blaskovich MA, Butler MS, Huang JX, Zuegg J, Mamidyala SK, Ramu S, Kavanagh AM, Cooper MA (2014) Bioorg Med Chem 22:4490
5. Butler MS, Blaskovich MA, Cooper MA (2017) J Antibiot 70:3
6. Zha G-F, Wang S-M, Rakesh K, Bukhari S, Manukumar H, Vivek H, Mallesha N, Qin H-L (2019) Eur J Med Chem 162:364
7. El-Kardocy A, Mustafa M, Ahmed ER, Mohamady S, Mostafa YA (2019) Med Chem Res 28:2088
8. Ghorab MM, Al-Said MS (2012) Arch Pharmacal Res 35:987
9. El-Din MMG, El-Gamal MI, Abdel-Maksoud MS, Yoo KH, Oh C-H (2015) Eur J Med Chem 90:45
10. Ghorab MM, Ragab FA, Heiba HI, Agha HM, Nissan YM (2012) Arch Pharmacal Res 35:59
11. Ghorab MM, Ismail ZH, Abdalla M, Radwan AA (2013) Arch Pharmacal Res 36:660
12. Arshad M (2018) Int J Pharm Sci Res 9:35
13. Lavanya R (2017) Int J Pharm Sci Invent 6:1
14. Askar F, Aldhalf Y, Jinzeel N (2017) Int J Chem Sci 15:173
15. Fathalla OA, Zaghary WA, Radwan HH, Awad SM, Mohamed MS (2002) Arch Pharmacal Res 25:258

16. Bahekar SP, Hande SV, Agrawal NR, Chandak HS, Bhoj PS, Goswami K, Reddy M (2016) Eur J Med Chem 124:262
17. Basanagouda M, Shivashankar K, Kulkarni MV, Rasal VP, Patel H, Mutha SS, Mohite AA (2010) Eur J Med Chem 45:1151
18. Uddin MJ, Rao PP, Knaus EE (2003) Bioorg Med Chem 11:5273
19. Pinney KG, Mejia MP, Villalobos VM, Rosenquist BE, Pettit GR, Verdier-Pinard P, Hamel E (2000) Bioorg Med Chem 8:2417
20. Agard NJ, Baskin JM, Prescher JA, Lo A, Bertozzi CR (2006) ACS Chem Biol 1:644
21. Meyer D, Smeilus T, Pliatsika D, Mousavizadeh F, Giannis A (2017) Bioorg Med Chem 25:6098
22. Van Ostrand R, Jacobsen C, Delahunty A, Stringer C, Noorbehesht R, Ahmed H, Awad AM (2017) Nucleosides. Nucleotides Nucleic Acids 36:181
23. Nasr T, Bondock S, Eid S (2016) J Enzyme Inhib Med Chem 31:236
24. Yun M-K, Wu Y, Li Z, Zhao Y, Waddell MB, Ferreira AM, Lee RE, Bashford D, White SW (2012) Science 335:1110
25. Lipinski CA (2000) J Pharmacol Toxicol Methods 44:235
26. Lipinski CA, Lombardo F, Dominy BW, Feeney PJ (1997) Adv Drug Deliv Rev 23:3
27. Daina A, Michielin O, Zoete V (2017) Sci Rep 7:42717
28. Martin YC (2005) J Med Chem 48:3164
29. Yang JJ, Ursu O, Lipinski CA, Sklar LA, Oprea TI, Bologa CG (2016) J Cheminform 8:29
30. Mustafa M, Anwar S, Elgamal F, Ahmed ER, Aly OM (2019) Eur J Med Chem 183:111697
31. Clinical and Laboratory Standards Institute (2015) Performance standards for antimicrobial susceptibility testing. In: 25th informational supplement, M100-S25, vol 35, no 3. CLSI, Payne